Chemically ordered $Al_xGa_{1-x}N$ alloys: Spontaneous formation of natural quantum wells

M. Albrecht*
Institut für Kristallzüchtung, Max-Born-Strasse 2, D-12489 Berlin, Germany

L. Lymperakis and J. Neugebauer
Universität Paderborn, Fakultät für Naturwissenschaften, Fachbereich 6-Physik, D-33095 Paderborn, Germany

J. E. Northrup
Palo Alto Research Center, Palo Alto, California 94304, USA

L. Kirste
Fraunhofer Institut Angewandte Festkörperphysik, Tullastrasse 72, D-79108 Freiburg, Germany

M. Leroux
Centre de Recherche sur l' Hetero-Epitaxie et ses Applications, CNRS, Rue B. Grégory, F-06560 Valbonne, France

I. Grzegory and S. Porowski
Polish Academy of Sciences, High Pressure Research Centre, Warsaw, Poland

H. P. Strunk
Universität Erlangen-Nürnberg, Institut für Werkstoffwissenschaften, Lehrstuhl Mikrocharakterisierung, Cauerstr. 6, D-51058 Erlangen, Germany

(Received 8 March 2004; revised manuscript received 6 October 2004; published 13 January 2005)

We combine transmission electron microscopy, high-resolution x-ray diffraction, cathodoluminescence, and photoluminescence experiments with first-principles calculations to study the formation, thermodynamic stability, structural, and optical properties of chemically ordered $Al_xGa_{1-x}N$ alloys ($0<x<1$). Our results reveal that group-III-nitride surfaces exhibit chemically highly sensitive adsorption sites at step edges and that these sites can be used to kinetically engineer chemically ordered $Al_xGa_{1-x}N$ alloys. The ordered alloys have unique properties: (i) the band gap is redshifted up to 110 meV with respect to the disordered alloy of the same composition and (ii) the band gap reduction is caused by localization of the band edge wave functions in the GaN layer. Ordered $Al_xGa_{1-x}N$ thus can be seen as a natural quantum well structure where electrons and holes are localized and confined in monolayer GaN quantum wells.

DOI: 10.1103/PhysRevB.71.035314 PACS number(s): 78.67.−n, 61.14.−x, 71.20.−b

I. INTRODUCTION

Optical properties of nitride-based ternary compounds ($Al_xGa_{1-x}N$, $In_xGa_{1-x}N$, $Ga_xAs_{1-x}N$) are distinguished from their classical arsenide- or phosphide-based counterparts (e.g., $Al_xGa_{1-x}As$, $In_xGa_{1-x}As$) by a number of anomalous optical properties such as a strong band-gap bowing and a large Stokes shift between absorption and emission. These anomalous properties have been related to strong localization of the carrier wave function at the scale of the elementary cell, which is a result of the strong dissimilarities of the constituents of the alloy, e.g., in band offsets (1.8 eV between AlN and GaN) and in lattice constants (~11% between InN and GaN). Exciton localization thus seems to be an intrinsic property of the alloy[1–3] and optical properties of these alloys depend on fluctuations *on the scale of the nearest-neighbor distribution*. Thus, even statistical fluctuations on the atomic scale (as unavoidable for homogeneous but random/disordered alloys) affect alloy properties. This effect has important implications for device design: It makes the formation of atomically sharp interfaces or of quantum wells with precise thickness principally impossible. The growth of nitride-based quantum wells with well-defined optical properties therefore requires a new way to control alloy fluctuations on an atomic level. The natural way to do this is to introduce order in form of monatomic superlattices into the alloy.

Experimental and theoretical studies[4–7] of ordering in III-V semiconductor alloys having the zinc-blende structure have been able to link the thermodynamics and growth kinetics with the optical properties of the alloy. And though the existence of ordering in wurtzite nitride alloys has been clearly established and studied by a number of authors[8–15], the corresponding link has not been elucidated until now. For wurtzite, the ordered alloy consists in most cases of a "monatomic" superlattice formed of single AlN (or InN) and GaN alternating along [0001] (Fig. 1). This ordering leads to reduction of the lattice symmetry from $P6_3mc$ to $P3mc$ but does not change the size of the unit cell. While ordering has been clearly observed no experimental information regarding the formation of the ordered structures (i.e., whether they are of kinetic or thermodynamic nature) or regarding their optical properties (compared to random alloys) are available.

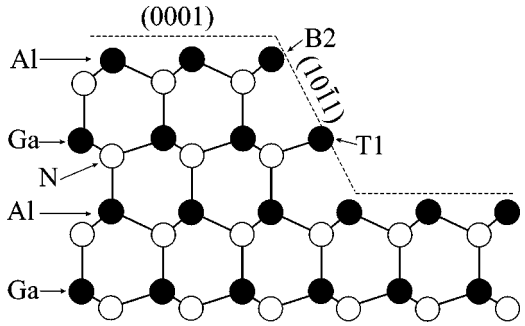

FIG. 1. Model of a monatomic superlattice consisting of alternating AlN and GaN layers. Group-III atoms at *B*2 (*T*1) sites form two (one) bonds with the N atoms in the layer below. Growth of ordered alloys may occur by preferential incorporation Al (Ga) at *B*2 (*T*1) sites at the exposed facet, and by the lateral movement of this facet across the surface.

In this paper we combine transmission electron microscopy and high-resolution x-ray experiments with first principles calculations to study structural and optical properties of ordered $Al_xGa_{1-x}N$ alloys ($0<x<1$). To compare the thermodynamic stability of ordered structures we perform annealing experiments at high temperature and high N pressure. We find that (i) ordered $Al_xGa_{1-x}N$ is thermodynamically unstable in the bulk. During growth it is induced at surface steps and caused by the different coordination of group-III atoms at the step edges. (ii) The cathodoluminescence of ordered $Al_xGa_{1-x}N$ alloys can be redshifted by up to 110 meV with respect to the disordered alloy of the same composition. (iii) The band gap reduction is caused by localization of the band edge wave functions in the GaN layer. Ordered $Al_xGa_{1-x}N$ may therefore be viewed as a natural quantum well structure where electrons and holes are localized in a monolayer GaN quantum well.

II. EXPERIMENTAL DETAILS

To perform the studies we have grown 700–785-nm-thick $Al_xGa_{1-x}N$ layers onto sapphire (0001) substrates by plasma-enhanced molecular beam epitaxy (MBE) in a Riber P32 machine equipped with gallium and aluminum effusion cells. Nitrogen radicals are produced by the OAR CARS25 radio frequency plasma source with a nitrogen flow rate of 1.4 sccm (standard cubic centimeters per minute) and a radio frequency power of 440 W. The $Al_xGa_{1-x}N$ layers were grown at a temperature of 800–850 °C. Prior to the $Al_xGa_{1-x}N$ layers, AlN buffer layers with a thickness of 100–200 nm were deposited at 1050 °C. The aluminum concentration of the resulting layers has been determined by high-resolution x-ray diffraction using the Extended Bond Method.[16] Subsequently the grown specimens have been cut into two pieces of which one of each pair has been subjected to annealing treatments (1350 °C, 9.5 kbar nitrogen pressure). From these specimens plane-view and cross-sectional electron transparent samples have been prepared by standard techniques including mechanical grinding and polishing followed by 4-keV Ar^+ ion milling. Transmission electron diffraction, dark-field images and high resolution electron microscopy has been performed in a Philipps CM 300 UT microscope operated at 300 keV. Transmission electron diffraction patterns have been recorded by a charge coupled device camera. The degree of order has been quantified by evaluation of the integral intensity ratio between the order sensitive 0001 superlattice reflection and the 0004 fundamental reflection.[24] Since electron diffraction is dynamical even for moderate sample thickness we have to account in addition for the sample thickness. We use the integral intensity ratio between the 0001 and 0003 reflection to determine the thickness since this ratio depends exclusively on the thickness and is insensitive to order (for details see Ref. 17).

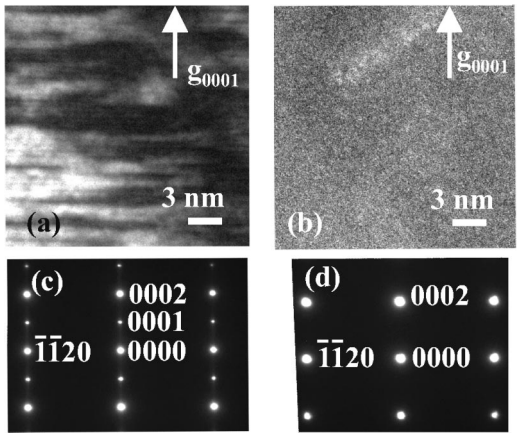

FIG. 2. (a) and (b) Distribution of order domains in $Al_xGa_{1-x}N$ ($x=0.56$) before and after annealing at high temperature and high pressure. Cross-sectional transmission electron dark-field images are taken with order-sensitive 0001 reflection under dark-field conditions [the corresponding electron diffraction patterns are shown in (c) and (d), respectively]. (a) Order domains in the as-grown samples appear bright. Dark areas are disordered regions. Clear 0001 spots can be seen in the electron diffraction pattern taken along $1\bar{1}00$. (b) No order is present after annealing, as indicated by the absence of the respective order spots in the electron diffraction.

III. RESULTS: STRUCTURE

A. Experiment

Figure 2(c) shows a typical transmission electron diffraction pattern of an $Al_xGa_{1-x}N$ sample ($x=0.56$) taken along the $[1\bar{1}00]$ zone axis. In addition to the wurtzite fundamental reflections, 0001 superlattice reflections can be seen, weaker in intensity than the fundamental reflections. These reflections are indicative of a monoatomic AlN—GaN superlattice along the [0001] direction (Fig. 1). Dark-field images using the 0001 superlattice reflection [Fig. 2(a)] reveal the presence of ordered and disordered domains: the highly ordered regions are discernible by bright intensity. These domains have a lateral extension ranging from 100 to 250 nm and a thickness (in the growth direction) between 3 and 10 nm. The size of these ordered regions increases from the interface between the $Al_xGa_{1-x}N$ layer and AlN buffer layer to the surface. It is interesting to note that together with the increase in size the ordering improves—the ordering param-

eter goes from $S=0.25$ (close to the interface) to $S=0.35$ (close to the surface).

Plane-view images show the presence of domain boundaries between ordered and disordered regions by a faint line contrast. The domains exhibiting ordering have trigonal shape and appear related to the surface topology: atomic force microscopy (AFM) measurements show that for the growth conditions applied in this study the surface is formed of hexagonal hillocks bound by $\{hh\bar{0}1\}$ surface facets. The inclination angle of the facets binding the hillocks is <3 with respect to [0001].

Samples having a wide range of Al compositions have been examined ($x=0.240$, 0.524, 0.564, 0.637, 0.787). We find, consistent with other studies,[9] that chemical ordering of varying degree is present for all of these compositions. Since we are interested in the monolayer superlattice formation with an Al concentration of $x=0.5$, the order parameter S has been quantified only for samples close to this composition. A maximum value close to $S=0.35$ has been found. Since electron diffraction is integrating over areas of 100 nm in diameter and 100 nm in thickness the order parameter is an average over ordered and disordered domains. Thus the order parameter will be higher than $S=0.35$ in the order domains themselves but cannot be measured because of the limited resolution of our diffraction method (100 nm).

Further insight into the formation of the alloys follows from our study of the thermodynamic stability. After annealing the sample for 5 h at 1350 °C and high nitrogen pressure (9.5 kbar) the 0001 reflections have disappeared and no indications for long-range order can be found in either the high-resolution x-ray diffractograms or the electron diffraction patterns [see Figs. 2(b) and 2(c), which show a dark-field image and an electron diffractogram taken along $\langle 1\bar{1}00\rangle$ after annealing]. The results of the x-ray diffraction Extended Bond measurements shows that the Al concentration of as-grown and annealed samples is identical, while the compressive stress in the layers is slightly increased after annealing. Annealing experiments have been performed for all samples: In all cases the order disappears upon annealing. We therefore conclude that the thermodynamic stable configuration of $Al_xGa_{1-x}N$ alloys is disordered: The formation of the ordered structures must be induced by kinetic growth processes.

B. Theory

1. Fundamentals

In order to explore possible mechanisms leading to ordering density-functional calculations in the plane-wave pseudopotential approach as implemented in the SFHINGX code[18] have been employed. Specifically, Troullier-Martin pseudopotentials,[19] a plane-wave cutoff of 70 Ry, and the Perdew-Berke-Ernzernot generalized gradient approximation to describe exchange and correlation have been used. An equivalent of $4\times4\times1$ Monkhorst-Pack k-point sampling for the unit cell has been applied. The ordered structures have been described in a 1×1 supercell where GaN and AlN layers alternate along [0001]. To represent disordered alloys within a supercell formalism (which intrinsically contains periodic boundary conditions), we considered a number of ordered structures that have been constructed in such a way that they mimic different local environments. Specifically, the chalcopyrite structure, the CuPt structure, and luzonithe structures have been considered and in the following are referred to as the disordered structure. For all structures the lattice parameters and internal coordinates have been fully relaxed.

2. Thermodynamic stability

Based on these structures the formation energy has been calculated as

$$E_f = E_{\mathrm{tot}}(\mathrm{Al}_x\mathrm{Ga}_{1-x}\mathrm{N\ alloy}) - xE_{\mathrm{tot}}(\mathrm{AlN}) - (1-x)E_{\mathrm{tot}}(\mathrm{GaN}), \tag{1}$$

with E_{tot} (AlN) and E_{tot} (GaN) the total energies of bulk AlN and GaN. Our results show that the formation energies of the disordered structures are identical within the margin of error (0.1 meV/cation) for these calculations. However, the 1:1 [0001] superlattice has a formation energy that is higher by 3.0 meV per cation. The somewhat higher formation energy in this case, where the layers are either all Al or all Ga, results from the uneven strain distribution. Since the covalent radius of Al is slightly smaller than that of Ga, there is a tensile strain in the Al layers and a compressive strain in the Ga layers. In disordered alloys, however, each layer contains an equal number of Al and Ga atoms and so the net strain becomes small. In addition, there is a reduction in free energy in the disordered structure arising from increased configurational entropy. This effect is significant at the growth temperature [of the order $\ln(2)k_BT\approx0.67k_BT$ for $x=0.5$] and favors the disordered structure. Thus, the theoretical results are in full accordance with our annealing experiments: the ordered structure is *thermodynamically unstable*.

3. Kinetically driven ordering

We have therefore studied whether a kinetic mechanism recently proposed for $In_xGa_{1-x}N$ alloys can be used to explain the ordering. According to this model,[20] the occupation statistics of metal atoms on the group III sublattice is governed by the local energy balance at the growth surface, consisting of $\{1\bar{1}01\}$ facets: Metal atoms at $B2$ sites in Fig. 1 are bound to two N atoms in the layer below, while the atoms in $T1$ positions are bound to only one N atom. In our case the Al—N bond is stronger than the Ga—N bond. Thus the system can minimize its energy during growth by incorporating Al atoms preferably on $B2$ sites where two N bonds can be saturated. We have performed density-functional theory (DFT) calculations for the $(1\bar{1}01)$ surface and find that the energy reduction obtained upon exchanging an Al atom bound to a $T1$ site with a Ga atom bound to a $B2$ site is 0.67 eV. This energy is large compared to k_BT at the growth temperature and therefore this mechanism provides a significant driving force for ordering.

It should be mentioned that the mechanism giving rise to order in the present case is quite different from that discussed for III-V zinc-blende alloys grown on the (001) surface: In

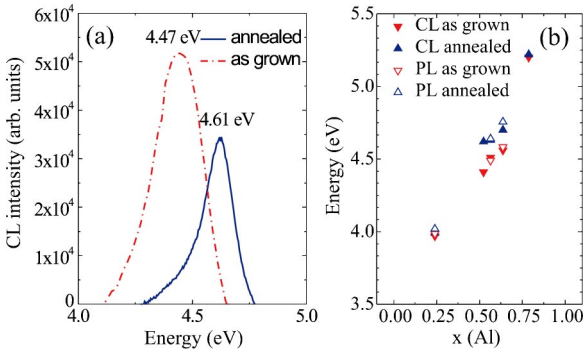

FIG. 3. (Color online) Photoluminescence (PL) and cathodoluminescence (CL) data of ordered and disordered $Al_xGa_{1-x}N$ samples. (a) Transmission electron microscopy cathodoluminescence spectra taken at 90 *K* of ordered (as-grown) and disordered (annealed) samples under identical excitation conditions. The CL peak of the ordered sample is redshifted but has an increased full width at half maximum. (b) CL peak position of ordered and disordered samples throughout the whole range of Al concentration. The redshift of ordered samples with respect to the disordered ones is maximum for an Al fraction around $x=0.5$.

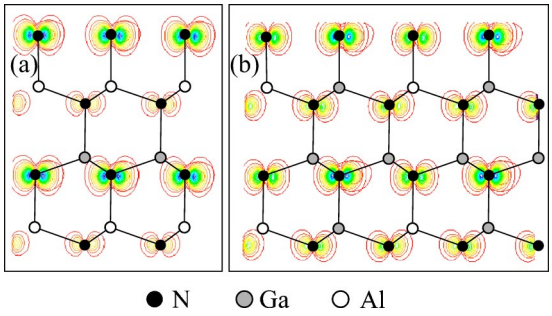

FIG. 4. (Color online) Contour plots of the valence band states in ordered and disordered $Al_xGa_{1-x}N$ ($x=0.5$). (a) For the 1×1 ordered structure a strong localization of the valance band state at N atoms bound to three Ga atoms (i.e., in the GaN layer) can be seen. (b) For the disordered sample the wave function is no longer confined to the GaN layer and thus more delocalized.

that case the order is thought to arise from the strain fields caused by surface dimers occurring in specific surface reconstructions (see, for example, Ref. 5). In contrast, formation of order in wurtzite semiconductors requires diffusion of adatoms to the step edges or vicinal facets, where they incorporate at preferred sites. This can be expected for high growth temperatures and low growth rates and fits well experimental observations by Ebling *et al.*[21]

IV. RESULTS: OPTICAL PROPERTIES

A. Experiment

The optical properties of ordered $Al_xGa_{1-x}N$ are discussed next. A comparison of the calculated band gap of the ordered and the disordered structures shows that the band gap of the 1×1 superlattice structure is reduced by 100 meV with respect to that of the various disordered structures, which all have the same band gap within the error of our calculation. Experimentally the effect of ordering on the optical properties has been studied by cathodoluminescence (CL) and photolumenescence (PL). Figure 3(a) shows cathodoluminescence spectra of as-grown (i.e., ordered) and annealed (i.e, disordered) $Al_xGa_{1-x}N$ samples with $x=0.56$. The CL peak position of the ordered sample shows a pronounced redshift of 140 meV with respect to the disordered sample. Furthermore the ordered sample shows an increased full width at half maximum (FWHM) and an increased CL and PL peak intensity compared to the disordered sample under identical excitation conditions. Figure 3(b) summarizes the cathodoluminescence peak positions of ordered and disordered samples throughout the whole investigated range of concentrations. As can be expected the redshift is most pronounced for the alloys around $x=0.5$.

B. Theory

Our calculations of the electronic structures performed for the various atomic structures indicates that the band gap for all of the disordered structures is 3.03 ± 0.01 eV, while that for the ordered structure is 2.95 eV. Thus, the calculated redshift arising from ordering is ~80 meV. This is lower than the experimental value of 140 meV, and agrees very well with the value of 90 meV obtained by Dudiy and Zunger[22] using a similar approach (DFT local density approximation). To explain the physical nature of the reduction in band gap with 1×1 ordering, we compare the valence band and conduction band wave function for the chalcopyrite (disordered) and for the 1×1 superlattice (ordered) structure. As can be seen from Fig. 4(a) the *p*-like valence band of the disordered structure is delocalized. In contrast to that, the valence band wave function of the ordered structure is localized at the N atom that is bound to three Ga atoms, i.e, in the GaN layer of the 1×1 superlattice. The same localized (delocalized) character has been found also for the *s*-like conduction band wave functions of the ordered (disordered) structures. This essentially resembles localization of electrons and holes in a monatomic GaN quantum well embedded in monatomic AlN barriers. The origin of band-gap reduction is thus carrier localization and not level repulsion due to Brillouin zone folding (the dominating effect in band-gap reduction of ordered zinc-blende semiconductors[5]). Brillouin zone folding does not occur in wurtzite since the present 1×1 ordering changes only the occupation of the unit cell, while the periodicity along the *c* axis is unchanged. In order to estimate the difference between the two mechanisms we performed additional calculations for ordered and disordered cubic $Al_xGa_{1-x}N$ alloys. The results are listed in Table I and are very similar to the wurtzite case: Ordering is thermodynamically unstable and the band gap increases by 60 meV when going from ordered to disordered structures.

V. CONCLUSIONS

From a combined experimental and theoretical approach we have shown that ordering in wurtzite $Al_xGa_{1-x}N$ alloys is introduced due to growth kinetics at surface steps and is caused by the energy difference of the bonds between Al—N and Ga—N. Ordering in nitrides, thus, requires a growth regime that allows adatoms to diffuse to the step

TABLE I. Calculated lattice constant, c/α ratio, and band gap for zinc blende (ZB) and wurtzite GaN, AlN, and $Al_{0.5}Ga_{0.5}N$ ordered and disordered alloys.

	Phase	α (bohr)	c/α	E_{gap} (eV)
GaN	wz	6.04	1.63	2.06
AlN	wz	5.90	1.60	4.13
$Al_{0.5}Ga_{0.5}N$ ordered	wz	5.97	1.62	2.95
$Al_{0.5}Ga_{0.5}N$ disordered	wz	5.97	1.62	3.03
GaN	ZB	8.53	—	1.86
AlN	ZB	8.31	—	4.06
$Al_{0.5}Ga_{0.5}N$ ordered	ZB	8.41	—	2.80
$Al_{0.5}Ga_{0.5}N$ disordered	ZB	8.42	—	2.86

edges, i.e., comparatively high growth temperatures and low growth rates, respectively. Once formed the order is extremely stable because of the low diffusion coefficients in nitride semiconductors. Ordering reduces the band gap due to localization in quantum-well-like states, i.e., ordered nitrides behave as a natural multi-quantum well structure. Since the degree of order can be controlled by growth temperature or growth rate, lattice-matched heterostructures consisting of ordered and disordered $Al_xGa_{1-x}N$ of the same composition become possible. This could be of interest, because one could completely reduce the piezoelectric fields in $Al_xGa_{1-x}N$-based quantum well structures. Moreover, ordered alloys could solve the problems that are caused by the change of symmetry from $\Gamma 9$ (for GaN) to $\Gamma 7$ of the valence band maximum for Al concentrations $x > 4\%$.[23] The change of the valence band symmetry, when going from GaN to AlN, is caused by the stronger ionicity of AlN. It causes a transfer of almost the entire optical oscillator strength at $k = 0$ for the fundamental band gap to π transitions, i.e., with the electrical field parallel to the c axis. Thus light emission along c is strongly reduced in structures with high Al concentrations, which is negative for surface-emitting devices. Ordering leads to a change in the sequence of the valence bands back to that found in GaN:[22] This is an interesting option, e.g., for vertical cavity surface-emitting lasers in the deep uv region.

ACKNOWLEDGMENTS

Work at Erlangen-Nürnberg University and at University of Paderborn (L.L. and J.N.) was supported in part by the European Union within the framework of the IPAM research and training network. Part of the electron microscopy investigation took place in the Central Facility for High-Resolution Electron Microscopy. L.K. thanks N. Herres for helpful discussions concerning the structural analysis of the layers. J.N. and L.L. thank the Deutsche Forschungsgemeinschaft (DFG research group "Nitride based QD lasers" University of Bremen). J.E.N. is supported in part by the U.S. Office of Naval Research. M.A. thanks A. Zunger for helpful discussions.

*Electronic address: albrecht@ikz-berlin.de

[1] L. Bellaiche and A. Zunger, Phys. Rev. B **57**, 4425 (1998).
[2] L. Bellaiche, T. Mattila, L.-W. Wang, S.-H. Wei, and A. Zunger, Appl. Phys. Lett. **74**, 1842 (1999).
[3] M. Gallart, A. Morel, T. Taliercio, P. Lefebvre, B. Gil, J. Allègre, H. Mathieu, N. Grandjean, M. Leroux, and J. Massies, Phys. Status Solidi A **180**, 127 (2000).
[4] K. A. Mäder and A. Zunger, Phys. Rev. B **51**, 10462 (1995).
[5] A. Zunger and S. Mahajan, in *Handbook of Semiconductors*, 2nd ed., edited by S. Mahajanvol (Elsevier, Amsterdam, 1994), Vol. 3.
[6] T. S. Kuan, T. F. Kuech, W. I. Wang, and E. L. Wilkie, Phys. Rev. Lett. **54**, 201 (1985).
[7] T. Y. Seong, G. R. Booker, A. G. Norman, and I. T. Ferguson, Appl. Phys. Lett. **64**, 3593 (1994).
[8] Z. Liliental-Weber, M. Benamara, J. Washburn, I. Grzegory, and S. Porowski, Phys. Rev. Lett. **83**, 2370 (1999).
[9] D. Korakakis, K. F. Ludwig, Jr., and T. D. Moustakas, Appl. Phys. Lett. **71**, 72 (1997).
[10] E. Iliopoulos, K. F. Ludwig, Jr., T. D. Moustakas, and S. N. G. Chu, Appl. Phys. Lett. **78**, 463 (2001).
[11] P. Ruterana, G. De Saint Jores, M. Laügt, F. Omnes, and E. Bellet-Amalric, Appl. Phys. Lett. **78**, 344 (2001).
[12] P. Ruterana, G. Nouet, W. Van der Stricht, I. Moerman, and L. Considine, Appl. Phys. Lett. **72**, 1742 (1998).
[13] D. Doppalapudi, S. N. Basu, and T. D. Moustakas, J. Appl. Phys. **85**, 883 (1999).
[14] M. K. Behbehani, E. L. Piner, S. X. Liu, N. A. El-Masry, and S. M. Bedair, Appl. Phys. Lett. **75**, 2202 (1999).
[15] M. Benamara, L. Kirste, M. Albrecht, K. W. Benz, and H. P. Strunk, Appl. Phys. Lett. **82**, 547 (2003).
[16] N. Herres, L. Kirste, H. Obloh, K. Köhler, J. Wagner, and P. Koidl, Mater. Sci. Eng., B **91–92**, 425 (2002).
[17] C. Eder, M. Albrecht, and H. P. Strunk (unpublished).
[18] See www.sfhingx.de
[19] N. Troullier and J. L. Martins, Phys. Rev. B **43**, 1993 (1991).
[20] J. E. Northrup, L. T. Romano, and J. Neugebauer, Appl. Phys. Lett. **74**, 2319 (1999).
[21] D. G. Ebling, L. Kirste, K. W. Benz, N. Teofilov, K. Thonke, and R. Sauer, J. Cryst. Growth **227–228**, 453 (2001).
[22] S. V. Dudiy and A. Zunger, Phys. Rev. B **68**, 041302(R) (2003).
[23] M. Leroux, S. Dalmasso, F. Natali, S. Helin, C. Touzi, S. Laügt, M. Passerel, F. Omnes, F. Semond, J. Massies, and P. Gibart, Phys. Status Solidi B **234**, 887 (2002).
[24] The degree of order for the 1×1 *ACBC* superlattice is quantified by the order parameter $S = 2r_A - 1$. Here r_A is the probability to find an atom of type A on an A site.